



MID-AMERICA TRANSPORTATION CENTER

Report # MATC-UI: 271

Final Report

UNIVERSITY OF
Nebraska
Lincoln

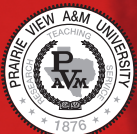
KSTATE
Kansas State University

KU
THE UNIVERSITY OF
KANSAS

MISSOURI
S&T
University of
Science & Technology


THE UNIVERSITY OF IOWA

 **LINCOLN**
University



Improving Freight Fire Safety: Assessment of the Effectiveness of Mist-controlling Additives in Mitigating Crash-induced Diesel Fires

Albert Ratner, Ph.D.

Assistant Professor

Mechanical and Industrial Engineering

University of Iowa



THE UNIVERSITY OF IOWA

2010

A Cooperative Research Project sponsored by
U.S. Department of Transportation Research and
Innovative Technology Administration

The contents of this report reflect the views of the authors, who are responsible for the facts and the accuracy of the information presented herein. This document is disseminated under the sponsorship of the Department of Transportation University Transportation Centers Program, in the interest of information exchange.
The U.S. Government assumes no liability for the contents or use thereof.

MATC

Improving Freight Fire Safety: Assessment of the Effectiveness of Mist-Controlling Additives in
Mitigating Crash-Induced Diesel Fires

Dr. Albert Ratner
Assistant Professor
Mechanical and Industrial Engineering
University of Iowa

Table of Contents

Abstract.....	ii
Executive Summary.....	iii
List of Nomenclature.....	v
Chapters	
1. Introduction.....	1
2. Drop Impact Experiments.....	4
2.1 Experimental Arrangement and Procedure.....	6
2.2 Results.....	9
3. Numerical Simulation of Drop Impacts.....	13
3.1 Numerical modeling – grid, boundary conditions and solution.....	13
3.2 Results.....	14
3.2.1 Drop Impact with the Static Contact Angle (SCA) model.....	14
3.2.2 Drop Impact with the Dynamic Contact Angle (DCA) model.....	15
4. Conclusions.....	17
References.....	19
Tables.....	21
Figures.....	22

Abstract

Adding long chained polymers to diesel has been proposed as a method to prevent crash fires by arresting the break-up of diesel fuel into a fine mist in transportation related accidents. The effect of such additives on the flow properties of diesel was investigated by studying the impact of poly-butadiene and diesel blend drops on a solid surface using high speed imaging. The addition of the polymer imparted shear-thinning behavior to diesel, and the base viscosities increased rapidly with polymer concentration. Four concentrations of the polymer were tested at three different impact speeds under atmospheric pressure. Maximum spread factors and spreading velocities of the drops were found to decrease with increasing polymer concentration. This suggests that polymer addition decreases the tendency of diesel to break into smaller droplets. A numerical model of a drop impact process is being developed using FLUENT 12, and will be used to study the non-Newtonian effects in the flow of diesel blended with polymers. Results of these experiments and numerical modeling can facilitate the development of polymers with specific properties to affect the flow of diesel in the desired range of strain rates.

Executive Summary

Most crash related fires in transportation occur due to the rapid ignition of a fuel mist that forms due to the intensity of the accident. Since it is known that pools of diesel burn relatively slowly, a possible way of mitigating such crash induced fires is to prevent misting by mixing long chained polymer based additives into diesel. Such polymers, still in the developmental stages, are intended to impart non-Newtonian viscosity (shear-thickening) to diesel in a shear range that is typical of accidents but does not otherwise affect the normal functioning of the fuel system. Such an increase of viscosity retards the break-up of a liquid into smaller droplets.

In order to test the effect of such polymer additives a commonly occurring polymer, polybutadiene, was added to diesel at four different concentrations. Viscosity measurements showed that the polymer imparted a shear-thinning property to diesel, and that the base viscosity of the different mixtures increased with increasing concentrations of the polymer. To study the effect of this non-Newtonian viscosity on the flow properties of the resulting mixtures, impact of drops of these liquids on a smooth surface was studied using high speed photography under atmospheric pressure. A drop hitting a dry surface at moderate impact speeds experiences a wide range of strain rates during the resulting deformation; hence, this can be a suitable tool to test the viscosity variations of the polymer-diesel blends. The experiments showed that for similar impact speeds and drop sizes, the maximum spread factor—defined as the ratio of the maximum spread diameter to the initial diameter of the drop—and the spreading speeds decreased with increasing concentration of the polymer. This occurs due to greater energy dissipation caused by the increasing viscosity of the liquids with higher polymer concentration—indicating that the drop tends to stay together and dispersion into smaller droplets would become difficult. Comparisons of the non-Newtonian drops were made with those of a Newtonian blend of glycerol and iso-butanol. However, significant variation in drop sizes and surface tension between the two types of liquids limited the conclusions from this comparison.

Even though the experiments provided useful insights regarding the effect of polymer additive on flow characteristics of diesel, it is not possible to identify a particular shear range in such tests. Hence, computational simulation of drop impacts becomes necessary as it lends great flexibility in studying a particular range of strain rates. It also allows the desired variation of liquid properties in order to study the resultant effects on quantities of interest— like spread factors, drop shape and spreading velocities—without actually doing tests. Numerical modeling of drop impact on a smooth surface has been carried out using FLUENT 12 and has been validated with the experimental data. As compared to the experimental data, some differences have been observed in the prediction of spread factors, and current work is focused on making the model more accurate. Once developed, the computational results on the behavior of non-Newtonian drops could be utilized in adjusting the chemistry of the polymers such that the desired properties could be obtained.

Current research has led to useful insights into the possible effects of polymer additives on flow characteristics of diesel and on the requirements of additives. With concurrent progress in polymer chemistry, prevention of crash-induced fires can be achieved.

List of Nomenclature

V_0 = Impact speed of the drop

D_{eq} = Equivalent drop diameter

D_L = Larger diameter of the drop

D_S = Smaller diameter of the drop

d = Drop spread diameter at a given time

t = Time measured from the instant of impact

d_{max} = Maximum spread diameter of a drop

d_{lam} = Diameter of the spreading lamella

$d_{cont.}$ = Diameter of the contact line

β = Spread factor

β_{max} = Maximum spread factor

t^* = Non-dimensional time

μ_{eff} = Effective viscosity of the liquid

μ_0 = Base or zero-shear viscosity of the liquid

$\dot{\gamma}$ = Strain rate

θ_s = Static contact angle

θ_D = Dynamic contact angle

V = Spreading velocity

σ = Surface tension of the liquid

Chapter 1 Introduction

Each year accident induced fuel fires in road and rail transportation, worldwide, not only cause severe damages to property, but also result in casualties to human life. As is often the case, these fires are particularly hazardous when they involve freight; fuel fires can rapidly engulf the transported material triggering massive secondary fires that result in increased fire intensity, toxic smoke, and often both. Hence, the importance of developing better technologies for transportation safety can never be over-emphasized. Luckily, both accident prevention and accident mitigation have seen significant strides towards minimizing such occurrences. Techniques like crash-proof vehicle design, robust fuel tanks, fire extinguishing, and passenger safety devices, like seat belts and air-bags, reduce the harm caused by accidents. However, in accidents involving heavy-duty transport vehicles, the intensity of the resulting fire can leave such devices ineffective and can also prevent rescuers from reaching those in need. For minimizing or preventing such crash-induced fires, it is crucial to examine new possibilities with the fuel itself—the root cause of this issue. Recent developments in polymer chemistry might hold the key in developing specific fuel additives to suit this purpose.

Even a highly flammable liquid like diesel burns relatively slowly if it is in the form of a pool. However, fine droplets of the same fuel burn vigorously and, by contrast, are easier to ignite. In vehicular accidents, the energy of the impact breaks open the fuel tank and forces the diesel out with such force that the fuel disintegrates into a fine mist. This fuel mist is easily ignited by a spark or a hot metal point, causing a fire that propagates rapidly through the air and creates a fireball. The fireball releases energy that burns anything in the vicinity; thus, avoiding this mist formation can avert large scale fires. New research is focusing on developing long-chained associative polymer based fuel additives that will prevent fuel misting in accidents, while otherwise not affecting normal engine and fuel system operation. When added to a solvent, like diesel, such polymers would impart non-Newtonian characteristics due to the linking/de-linking of the polymeric chains under shear. Consequently, the resulting mixture would exhibit

viscosities dependent on shear stresses acting on the liquid. If a polymer could be developed that becomes active and imparts higher viscosity to the fuel in the shear range typical of accidental conditions, misting of the fuel could be reduced since it is more difficult to atomize liquids with higher viscosities. For this purpose, concentrated efforts are required not only in polymer chemistry, but also in fuel system analysis. Developing reliable experiments and computational models to provide feedback is essential to furthering polymer engineering. Ongoing research at the University of Iowa has focused on both fuel system analysis and developing computational models supported by simple tests. This report discusses the experimental and simulation details along with highlighting the conclusions that can be drawn from the work thus far.

Preliminary analysis of representative fuel systems has shown that there is a target range of fluid shear in which the polymer additive could be active. This range includes many accident conditions and avoids the fuel operating conditions. Since the main idea rests on activating the polymer in order to vary the viscosity of the liquid in the regime of interest, experiments must enable an easy variation of shear stresses to study its effect on liquid viscosity. Impact of liquid drops on a smooth surface provides an excellent tool for this purpose. When a drop of a liquid hits a dry solid surface, it deforms from an initial spherical shape to a final thin disk like shape over a matter of milliseconds. Due to this rapid deformation, strain rates from zero to as high as 10^6s^{-1} occur in such impacts. This spreading (or splashing) of drops upon impact is inherently tied to the viscosity and other critical fluid properties. By studying the spreading characteristics of drops of fuel-polymer blends using high speed photography, valuable insights can be obtained on the effect of the polymer additive on liquid properties. In the present experiments, drops of diesel blended with poly-butadiene (a commonly used polymer) have been tested for different concentrations of the polymer. This allows for an assessment of changes in the properties of diesel and its resultant effect on features like drop shape during deformation, spreading speeds, etc.

Concurrent to these experiments, numerical analysis of drop impacts were conducted using FLUENT 12 to simulate experimental conditions. An accurate numerical model would

lend immense flexibility in investigating the effect of varying the properties of the test mixtures without having to actually perform the tests. The data from the tests of diesel-polybutadiene blend have been used to validate the numerical model. The computational simulations enable easy identification and analysis of a particular range of shear stresses in a deforming drop that is otherwise difficult in actual experiments. The simulation results can then be feedback for developing polymers with specific properties that can influence the regime of interest. The effect of the new polymers on the fuel can then be tested: first on a small scale using the drop impact experiments, and then through full scale testing.

The current report first presents a description of the drop impact experiments and a discussion of its results. This is followed by the details of the computational model and its comparison with the available experimental data set. The report concludes with a discussion of the implications of the results obtained and the scope of future work to be done.

Chapter 2 Drop Impact Experiments

As mentioned in the introduction, spreading liquid drops on a smooth surface was selected as the tool for testing the effect of polymer additives on the flow properties of the resulting fuel mixture. During the impact of a liquid drop on a solid surface, the drop can either spread from an initial spherical shape to a thin disk like shape, or splash into droplets. The outcome is dependent on a number of factors such as viscosity, surface tension and density of the liquid, drop speed and size, nature of the impact surface, its surface roughness and temperature, and the surrounding gas. For example, liquids with high viscosity or surface tension show lesser spreading compared to those with lower values of these properties. High impact speeds or drop sizes result in larger spreading diameters and could also result in splashing if the kinetic energy is sufficiently high. Similarly, impacts on a rough surface show greater tendency to splash compared to those on smooth surfaces. For a given impact surface, impact speed and drop size, a comparison can be made between the properties of the liquids based on the spreading of their drops. In the present study, impacts of drops of diesel and polymer-diesel blends on a smooth surface have been studied under conditions well below the splashing threshold.

A sequence of a drop spreading on a solid surface is shown in figure 2.1. In the initial stage of a drop impact, a thin layer of liquid moves radially at speeds that can be several times higher than the impact speed. This layer of liquid is called a lamella and its thickness can be as low as a hundredth of the drop diameter. Surface tension and viscosity of the liquid quickly decelerate the lamella causing it to thicken. With time, the diameter of this spreading lamella attains a maximum, after which, depending on the nature of the liquid, it can spread further as a very thin film at much slower speeds, recoil, or become static. This entire process of spreading up to the maximum diameter occurs in a few milliseconds. Accordingly, high speed photography becomes important in studying such impact processes. The ratio of the diameter of the spreading liquid at any time instant after impact, and the initial drop diameter is called the spread factor β ; at the maximum spread diameter, the ratio is called the maximum spread factor β_{max} . The

variation of maximum spread factor has been used as a parameter for comparison between the properties of the liquid mixtures tested in the current experiments. The rate of spreading is another quantity that can yield useful insights into the effect of changes in the liquid properties. For example, for impacts with similar drop speed and size, a high viscosity liquid is expected to show lower spreading velocities. The present experiments have investigated these quantities.

As stated earlier, the addition of polymers imparts non-Newtonian characteristics to an otherwise Newtonian liquid and the viscosity of the resultant mixture becomes shear-dependent. The effective viscosity μ_{eff} of such liquids is commonly given by a power-law relation:

$$\mu_{eff} = \mu_0 \dot{\gamma}^{n-1}$$

If $n > 1$, the fluid is shear-thickening--that is, its viscosity increases with strain rate. On the other hand, for $n < 1$, the liquid is shear-thinning as its viscosity decreases with increasing strain rates. In a drop impact process, the drop experiences severe deformation over a small time-period and, as a result, the strain rates can be very high. For a drop 1 mm in diameter and impacting at a speed of 1 m/s, strain rates as high as 10^6s^{-1} can occur in the initial stage of deformation while the strain rates are close to zero near the maximum spread diameter. Hence, a spreading drop exhibits a wide range of strain rates and thereby the viscosity of a non-Newtonian liquid could be expected to vary during the spreading process. As compared to a Newtonian liquid under similar impact conditions, the effects of this non-Newtonian viscosity may be manifested as differences in contact line speeds and spread diameters. This is the basic premise for the present tests. The following section describes the experimental arrangement and procedure employed for the drop impact tests.

2.1 Experimental Arrangement and Procedure

The experimental arrangement is shown in figure 2.2. A quartz table smoothed to $0.2 \mu\text{m}$ Ra and fixed inside a pressure chamber was used as the impact surface. A blunt-end hypodermic needle enclosed in clear PVC tubing was used to generate and release drops from variable heights. Test liquid was supplied to the needle from an overhead reservoir through a PVC pipe

with a needle valve to control the flow through the needle. The chamber could be pressurized to the desired level using nitrogen gas supplied from compressed gas cylinders. Since, the present tests were carried out at atmospheric pressure, the chamber lid was kept open and the needle was held in position using fork clamps. An IDT XStream-Vision XS-3 digital camera was used for imaging the impacting drops almost normal to the direction of incidence. Impacts were recorded against a bright background created by a projector lamp to obtain very clear images of the deforming drop.

For this experiment, Poly-butadiene 140 ND (Molecular weight ≈ 300000) was blended in diesel at four different concentrations using a magnetic stir bar. The concentrations used were 0.5%, 1.0%, 1.4% and 2.0% of polymer in diesel, by weight. It was observed that with increasing concentration, the base viscosity of the solution increased significantly. However, since base viscosities of the blends were significantly different from each other, a comparison amongst the impact results of these diesel-polymer blends would not yield meaningful results. Therefore, these non-Newtonian drops were compared to drops of a Newtonian mixture with viscosities similar to the base viscosities of the corresponding polymer-diesel mixture. Since viscosity of a Newtonian liquid remains constant with strain rate, while it changes for a non-Newtonian liquid, such a comparison is expected to reveal the differences between the two kinds of impacts. The Newtonian blends were prepared by mixing 99.8% pure glycerol in isobutanol at different concentrations of glycerol. Viscosities were measured using a Brookfield Cup and Cone type viscometer as described later in this section. Isobutanol was chosen as the solvent since its properties are similar to diesel—as shown in table 2.1—and glycerol is readily soluble in it. The Newtonian drops were tested under the same conditions as the polymer blends and then comparisons were made between the two types of blends for each corresponding concentration.

Liquid viscosities were measured using a LV-series DV-II Brookfield Cup and Cone type digital viscometer. As the name suggests, the viscometer mainly consisted of a cup with a flat surface, and a cone which could be rotated at six different constant speeds using a synchronous motor. The working principle of such a viscometer states that when a test liquid is sheared

between a cone with small θ , as shown in figure 2.3, and a plate at a constant angular speed, the fluid experiences a uniform shearing stress in all regions. The ratio of this shear stress to the strain rate gives the viscosity of the liquid at that shear stress. For the present case, viscosities could be directly read off from the digital display. The viscometer was first calibrated using a standard liquid with a known viscosity at room temperature. Calibration was done to within 1% of the specified value. After calibration, viscosities of all samples of the diesel-polymer blend were measured. Due to the specifications of the viscometer, for a given liquid, it was possible to measure viscosities only at three angular speeds. Once a measurement was complete, plots of viscosity versus strain rate, as shown in figure 2.4, were generated and power law curves were fitted as best fit curves. The coefficient in the power-law equation of the curve was taken as the “zero-shear” or base viscosity of that sample. After this, mixtures of glycerol and iso-butanol were prepared using a trial and error process in order to obtain Newtonian liquids with viscosities similar to the base viscosities of the polymer-diesel blend. A plot of the variation of viscosity with glycerol concentration for glycerol-isobutanol mixtures is shown in figure 2.5. Through repeated trials, glycerol concentrations for the desired Newtonian viscosities were derived. Table 2.2 lists the different concentrations and their measured viscosities for both types of liquids.

Once the corresponding mixtures for the two types of liquids were prepared, impact tests were carried out under atmospheric pressure at identical impact speeds for both types of liquids. Impacts were obtained at three different impact speeds—0.7 m/s, 1.2 m/s and 1.6 m/s— by varying the height of the needle. Ten to fifteen drops of each liquid blend were recorded by manually triggering the camera for each impact speed. For every drop, the impact surface was cleaned using acetone and wiped dry with lintless lens tissues. Once the images were obtained, drop size and spread diameters were read off the screen in pixels and converted to millimeters using a calibration factor calculated from the image of a millimeter scale taken at the same camera focus as the drops. The calibration factor was obtained in mm/pixel by dividing the distance (in mm) between two extreme graduations visible in the image of the scale by the pixels

separating them--as read from the screen. Drop diameters were obtained by measuring pixel distance between two diametrically opposite points. Since the drops were not perfectly spherical, diameters were measured along both the horizontal and vertical axes. Assuming symmetry in the azimuth direction, the drop was considered as an ellipsoid for which an equivalent diameter D_{eq} was calculated as $D_{eq} = (D_L^2 D_S)^{1/3}$. This diameter, in pixels, was converted to millimeters by multiplying with the calibration factor. Spread factors for a deforming drop could be calculated at a given time instant after impact by dividing the spread diameter at that instant by D_{eq} . As shown in figure 2.6, spread diameters were calculated using the diameter of the lamella d_{lam} , instead of the contact line diameter d_{cont} . This is because the location of the contact line could not be precisely determined due to the limitations of the photography technique.

Impact speed was obtained by dividing the distance travelled by a drop in the last two frames prior to impact, by the time interval between the two frames. Spreading velocities for a given drop impact were calculated at each time instant by dividing half the change of spread diameter between two successive frames, with the time interval between the two frames. That is:

$$V_k = \frac{(d_{k+1} - d_k)}{2 * \Delta t}$$

where, k denotes the current frame, V_k denotes the spreading velocity at the time instant corresponding to frame k , d_k is the spread diameter in the current frame, d_{k+1} is the spread diameter in the next frame and Δt is the time interval between successive frames depending on the frame speed used.

Since, there were variations in the values of the quantities measured, an average value of parameters like drop diameter, impact speed and maximum spread factors was calculated by taking the arithmetic mean of all values of that parameter under a particular condition. Error bars were then created using standard deviation of the data set to judge the preciseness of the tests. All data have been reported at a 95% confidence level.

$$\bar{x}_i = \frac{1}{N} \sum_{i=1}^N x_i$$

MS-Excel was used to tabulate, calculate and plot the different sets of results which are presented in the following section.

2.2 Results

As mentioned previously and shown in table 2.2, the base viscosities of the diesel-polymer blend increased by about ten times from the lowest to the highest concentration of the polymer. For a given liquid blend, a variation of less than 1% was noted in the equivalent drop diameter. Drop distortion, measured as the difference between D_L and D_S , was less than 3% of the equivalent diameter, D_{eq} . Measurement of maximum spread factors β_{max} showed a variation of 1% for a given liquid. However, it was noted that even with the same needle size, an increase of about 7% occurred in drop size with an increase of polymer concentration from 0.5% to 2.0%. This increase could be attributed to the visco-elastic properties associated with the polymers, a fact that has been mentioned in published works on impact of non-Newtonian drops. A plot of the variation of β_{max} with impact speed for all concentrations of the polymer is shown in figure 2.7. As can be seen, for each concentration β_{max} increases with increasing impact speed due to increasing kinetic energy of the impacting drops. β_{max} decreases with increasing concentrations of the polymer since increasing viscosity of the blends with polymer concentration causes greater energy dissipation and hence lower β_{max} . The lower spread factors suggest that the drop tends to stay together, which means that breaking it into smaller droplets would be difficult.

An indication of the effect of liquid properties, like viscosity, on drop spreading can also be obtained by examining the rate of drop spreading. For a given drop size and impact speed, the greater the viscosity, the lower the rate of spreading should be due to viscous damping. A plot of the average spreading velocities for diesel drops ($D_{eq} = 2.15$ mm) at two different impact speeds is shown in figure 2.8. It is evident that the spreading velocities for the drop with a higher impact speed ($V_0 = 1.6$ m/s) are greater than that with a lower impact speed ($V_0 = 0.7$ m/s). For both drops, spreading velocities are significantly higher than the impact speed in the initial stages of drop spreading. However, the spreading velocities quickly reduce to the order of impact speed because of viscous effects. From figure 2.8, it is clear that the variation of the spreading

velocities can be described by a power-law curve. Similar results about contact line speeds have been reported by Engel (1) and Jepsen et al. (2).

As before, the addition of polymers to diesel resulted in a significant increase in the viscosity of the blend. This increase in viscosity caused a decrease of maximum spread factors for blends with higher concentration of polymer. A plot showing the variation of non-dimensional spreading velocity with non-dimensional time t^* ($= tV_0/D_{eq}$) is shown in figure 2.9 for two blends with polymer concentrations of 1% and 2%. The impact speeds for both the cases were nearly 1.2 m/s, while the drop diameters varied between 2.15 – 2.28 mm. The data points for spreading velocities in both figure 2.8 and figure 2.9 show a step-like variation with time for each liquid, especially for $t^* > 0.2$. This is because the calculations for spreading velocities were done using discrete frames, separated by a definite time interval. Thus, the minimum resolution for the measurement of speeds corresponded to one camera frame; any change lower than that could not be measured. This resulted in an uncertainty of nearly 0.07 m/s in speed measurements. Considering these uncertainties, it can be concluded from figure 2.9 that the spreading velocities are higher for the blend with 1% polymer concentration. This is due to the fact that the 1% solution had a lower base viscosity compared to the 2% solution. It is interesting to note that for spread time $t^* < 0.1$ no difference is observed between the two cases, despite the significant difference in the liquid viscosities; however, the two trend lines start diverging for $t^* > 0.1$. This suggests that viscosity does not affect the drop deformation process in the earliest part of spreading. However, it retards the flow in ‘spreading phase,’ that is, for $t^* > 0.1$. This result is a further validation of the findings of Rioboo et al. (3), who suggest that spreading is independent of liquid and surface properties in the initial phase of drop spreading.

Thus, the differences in viscosities of the test liquids are manifested in the behavior of contact line speeds and the spread factors. The above discussed results however, do not delineate the non-Newtonian effects, as the changes seen are due to the significant differences in base viscosities of the liquids tested. Therefore, the diesel-polymer blends were compared to Newtonian mixtures of glycerol and isobutanol (which has viscosities similar to the base

viscosities of the former). For nearly equal drop sizes and impact speeds, the differences between the two cases should be caused by the viscosity variation of the non-Newtonian drops. Such a comparison would help characterize the non-Newtonian effects in such drops.

Figure 2.10 shows a comparison of the β_{max} values for diesel and pure isobutanol at similar impact speeds. Due to the slightly lower surface tension of isobutanol, its drop size is about 5% lower than that of diesel. However, the viscosities of the two liquids were nearly identical, and for similar impact speeds, the maximum spread factors for the two liquids are also nearly identical. Thus, the spreading behavior of diesel and isobutanol could be assumed as reasonably similar. This ensures that, any change observed between the non-Newtonian and the Newtonian blends results from the addition of polymers and glycerol respectively, and does not stem from the parent liquids.

The Newtonian mixtures were tested at similar impact speeds as the corresponding non-Newtonian blends and a comparison was made for the spread factors and spreading velocities. Figure 2.11 shows a comparison of β_{max} for 1.4% polymer in diesel with the corresponding Newtonian blend—36.1% glycerol in isobutanol. The spread factors for the glycerol-isobutanol mixture are about 8% lower than those for diesel-polymer blend. This might indicate that, as expected, the viscosity of the non-Newtonian drop reduces due to high strain rates during impact, and hence gives it a greater spread than the Newtonian drop, whose viscosity remains constant. However, the difference in drop sizes for the two kinds of liquids needs to be accounted while analyzing this result. It was observed that, for the same needle size, the average size of the drop for the glycerol-isobutanol mixture was around 2.00 mm, whereas the polymer-diesel blend had average drop sizes at nearly 2.25 mm. It is possible that this 11% decrease in drop size might have resulted in lower β_{max} for the Newtonian liquid, but the value of surface tension was not measured for the two kinds of liquid. A significant difference in the values of surface tensions can also contribute to variations in spread factors.

Figure 2.12 shows a comparison of the evolution of spread factors with non-dimensional time for the two mixtures. The final spread factor for diesel-polymer blend is greater than the

glycerol-isobutanol mixture, as shown in figure 2.11. The two curves overlap in the initial part of spreading, for $t^* < 0.6$. After that, the rate of increase of spread factor for diesel-polymer mixture decreases slightly compared to the glycerol-isobutanol mixture. The curve for the glycerol-isobutanol mixture shows a dip after reaching a maximum value. This dip is due to a rapid change of contact angle occurring at the maximum diameter, and a strong reflection wave that reduces the lamella diameter d_{lam} as shown in figure 2.13. As was discussed earlier, d_{lam} was used to measure the spread factors rather than the contact line diameter d_{cont} . The final spread diameter was derived from the diameter of the contact line at equilibrium. For the diesel-polymer drops, this change of contact angle was more gradual and, consequently, no dip is observed in its curve. This difference in behavior of the two drops may be relative to the possible difference in the surface tension of the two mixtures.

Finally, a comparison of the average spreading velocities for the two liquid blends is shown in figure 2.14. It is apparent that the non-dimensional spreading velocities are similar for the two cases. No effect of non-Newtonian viscosities is evident from this velocity comparison. It is possible that such effects were suppressed due to the differences in drop sizes, and possibly, surface tension values between the Newtonian and the non-Newtonian liquids used.

Though this initial comparison between a non-Newtonian and a Newtonian blend could not lead to any conclusive evidence about effects of variable viscosity in a drop spreading process, it was shown that even small concentrations of a polymer can greatly change the properties of diesel. Viscosity measurements showed that the polymer-diesel blends indeed developed non-Newtonian characteristics. It was found that the initial part of the drop spreading process is unaffected by properties of the liquid, as previously noted by Rioboo et al. (3) In addition, a valuable data set has been generated for the validation of the numerical model of a drop impact process.

Chapter 3 Numerical Simulation of Drop Impacts

Liquid drop impact experiments with a blend of poly-butadiene in diesel provided some useful observations on the response of diesel to such polymers. However, in such experiments it is not possible to estimate the strain rates and the shear stresses experienced by the deforming drop at a given time instant. Therefore, numerical modeling becomes an essential tool to enable the analysis of strain rates, viscosities, shear stresses and other quantities of interest in the drop spreading process. As stated earlier, an accurate numerical model would lend great flexibility in modifying the properties of the test liquid and studying its effect on the spread diameters and spreading velocities. Hence, numerical modeling of drop impacts has been carried out using FLUENT 12 with the prime objective of developing a model that can predict the experimental results with reasonable accuracy.

3.1 Numerical Modeling: Grid, Boundary Conditions and Solution

A drop impact process is an example of an unsteady flow with forming interfaces and moving contact lines. Since a deforming drop involves an interface between the air and the liquid, Volume-of-Fluid (VOF) method has been used in FLUENT to carry out a 3-D modeling of the impact of a liquid drop on a solid wall in Cartesian coordinates. Modeling of the computational domain was carried out using GAMBIT. To minimize demands on computational resources without jeopardizing the ability to capture key features, the solution domain was restricted to a quarter of the full drop. With the knowledge of the initial diameter and the maximum spread diameter of the drops from the experiments, a domain measuring $6 \times 6 \times 5$ mm in x, y and z directions respectively, was chosen to represent a quarter of the total size. Since the thickness of the spreading lamella is of the order of 0.1 mm, a structured grid with refinement near the wall was used for discretizing the domain as shown in figure 3.1. The minimum thickness of the element used was 20 microns.

The boundary conditions applied on the different faces of the computational domain are shown in figure 3.1. No-slip boundary condition was specified at the wall where all the

components of velocity were set to zero. Two planes were set to a symmetry boundary condition, while all the remaining faces were defined as a pressure inlet. The Pressure Implicit with Splitting of Operator (PISO) was used for pressure velocity coupling in the momentum equation. The mass and momentum equations were solved using the QUICK scheme while the temporal derivatives were discretized using a first-order implicit method.

At the beginning of a simulation, a spherical drop was patched at the corresponding position in the computational domain. The patched zone was initialized with an impact velocity equal to the experimental velocities in the vertically downward direction. Time-steps of magnitude varying from 0.075 to 0.248 ms were used, and were equal to the time interval between successive frames of the experimental images taken at different camera speeds.

3.2 Results

3.2.1 Drop Impact with the Static Contact Angle (SCA) Model

The dynamics of a diesel drop with different velocities impacting on a horizontal surface, for which experimental measurements are available, was investigated. For the 2.16 mm diameter diesel drop with initial velocity of 1.6 m/s, the images of the evolution of drop shapes at different times for the static contact angle (SCA) model are shown in figure 3.2. (SCA = 17.9°) Static contact angle refers to the angle between the solid surface and a tangent that is drawn to the liquid-air interface at the contact line under static equilibrium. This angle is measured on the liquid side. A quantitative comparison of the measured and the simulated spread diameters is shown in figure 3.3. For dimensionless time $t^* < 0.8$ drop spreading is nearly identical for both the SCA model simulation and the experimental results, but an appreciable change of the shape starts from $t^* = 0.8$ onwards. In a drop spreading process, the contact angle varies from an initially high value to the final static value of the contact angle over the entire spreading process. As stated by Sikalo et al. (4), the spreading of a drop is independent of contact angles in the initial stages of splashing--this explains the similarity between the two results for $t^* < 0.8$. However, beyond this non-dimensional time spreading is affected by surface wettability effects;

thereby the SCA model is not sufficient to accurately predict the spreading process. Hence, a model based on dynamic contact angles needs to be applied.

3.2.2 Drop Impact with the Dynamic Contact Angle (DCA) Model

In order to predict the spreading diameters more accurately, a dynamic contact angle (DCA) model is necessary for the simulation. Sikalo et al. (4) reported a numerical study for drops impacting over flat surfaces by using modified Kistler's model (5). By applying stepwise time variation of the contact angle, Gunjal et al. (6) presented the observed variation during the drop impact process. A classical empirical equation was proposed by Jiang et al (7) which predicts the dynamic contact angle θ_D in terms of the capillary number ($Ca = \mu V / \sigma$) based on the contact line speeds, and the static contact angle θ_s .

$$\frac{\cos \theta_s - \cos \theta_D}{\cos \theta_s + 1} = \tanh(4.96Ca^{0.702})$$

The dynamic contact angles for spreading in the drop impact experiments were measured using the images of the drops. A comparison of the measured values with the angles predicted by Jiang's model is shown in figure 3.4 for a 2.16 mm diesel drop impacting the surface with a speed $V_0 = 1.6$ m/s. Calculations for Jiang's model are performed by using the velocity of spreading for the lamella. It can be seen that for $t^* < 0.6$, the measured contact angles show a nearly constant value of around 130° , whereas the values predicted by Jiang's correlation decrease with time. Beyond $t^* = 0.6$, the trends of the experimental contact angles and the theoretical angles show reasonable agreement. Figure 3.5 shows the variation of dynamic contact angles for diesel drops of roughly 2.16 mm in diameter at three impact speeds. All three cases exhibit two distinct regions θ_D , as mentioned earlier. However, the non-dimensional time marking the change from one region to the other shows dependence on the impact speed. Even though the maximum value of θ_D remains nearly same for the three speeds, the transition from region I to region II occurs earlier for low impact speeds.

Based on the above comparisons, a new model for specifying the dynamic contact angles is necessary for greater accuracy in describing the shape of the drop spread upon impact. Work is

currently under progress on the development of this model. Additionally, a User-defined Function (UDF) is being written to specify the contact angles for a more accurate prediction of the spread diameters.

Chapter 4 Conclusions

Impact of drops of a blend of poly-butadiene and diesel on a smooth and dry quartz surface were studied to investigate the effects of such polymer additives on the flow properties of diesel. It was noted that even at small concentrations of the polymer, there was an appreciable change in the properties of diesel, and the resultant mixture showed non-Newtonian viscosity behavior. This observation shows that long chained polymers can be used to modify specific properties of a fuel. Also, such polymers could be used at small concentrations to alter specific properties of alternate fuels so as to make them suitable for the fuel systems in use for conventional fuels, like diesel.

For this study drop impacts were obtained at three impact speeds for diesel-polybutadiene blends at four different concentrations of the polymer. It was seen that viscosity of the resultant mixtures increased with increasing polymer concentration causing lower spread factors and spreading velocities. The greater energy dissipation caused due to increasing viscosities retards the break-up of diesel drops into finer droplets. This is an important requirement for an anti-misting additive. Comparisons of diesel-polymer blend with a Newtonian blend of isobutanol and glycerol could not yield enough evidence of the effects of non-Newtonian viscosities in the spreading of the drops of diesel-polymer blends due to significant differences in drop sizes and surface tension of the two liquids. Future experiments ensuring uniform drop sizes and similarity in properties, like surface tension, could reveal the differences in the spreading behavior of the two liquids more clearly. Despite these limitations, the drop impact tests provided a useful data set for the validation of a drop impact process simulation.

Drop impact simulations using FLUENT 12 showed some disagreement between the spread factors obtained experimentally and those predicted by the computational model. This is because the simulations were carried out using a constant value of the contact angle (the static contact angle) which is not the case for actual drops where the contact angles vary throughout the spreading process. Thus, the current study is focused on improving the numerical model by

imposing more realistic values of the contact angles based on the measurements of dynamic contact angles observed in the impacts of diesel drops on the quartz surface.

Based on the studies so far, it can be said that addition of long chained polymers to diesel would prove effective in retarding its tendency to form a mist. However, the real challenge lies in developing polymers that would act in specific regimes of strain rates such that they do not affect the normal functioning of the fuel systems. With concurrent progress in flow analysis and polymer chemistry, achieving this objective appears to be a reality.

References

1. Engel, O.G., "Water drop collisions with solid surfaces." *Journal of Research of the National Bureau Standards* 54. 5 (1955).
2. Yoon, S.S., R.A. Jepsen, and B. Demosthenous. "Effects of air on splashing during a large droplet impact: Experimental and numerical investigations." *Atomization and Sprays* 16.8 (2006): 981-996.
3. Rioboo, R., M. Marengo, and C. Tropea. "Time evolution of liquid drop impact onto solid, dry surfaces." *Experiments in Fluids* 33 (2002): 112-124.
4. Sikalo, S., H.D. Wilhelm, I.V. Roisman, S. Jakirlic, and C. Tropea. "Dynamic contact angle of spreading droplets: Experiments and simulations." *American Institute of Physics, Physics of Fluids* 17 (2005).
5. Kistler, S.F., "Hydrodynamics of wetting." In *Wettability*, edited by J.C. Berg, 311. New York: Marcel Dekker, 1993.
6. Gunjal, P.R., W. Ranade, R.V. and Chaudhari. "Dynamics of drop impact on solid surface: Experiments and VOF simulations." *AIChE Journal* 51.1(2005): 59-78.
7. Jiang, T., S. Oh, and J.C. Slattery. "Correlation for dynamic contact angle." *Journal of Colloidal Interface and Science* 69(1979).
8. Rafai, S., D. Bonn, and A. Boudaoud. "Spreading of non-Newtonian fluids on hydrophilic surfaces." *Journal of Fluid Mechanics* 513(2004): 77-85.
9. Betelu, S.I. and M.A. Fontelos. "Capillarity Driven Spreading of Power-Law Fluids." *Applied Mathematics Letters* 16 (2003): 1315-1320
10. Rozhkov, A., B. Prunet-Foch, and M. Vignes-Adler. "Impact of drops of polymer solutions on small targets." *American Institute of Physics, Physics of Fluids* 15.7(2003).
11. Rozhkov, A., B. Prunet-Foch, and M. Vignes-Adler. "Dynamics and disintegration of drops of polymeric liquids." *Journal of non-Newtonian Fluid Mechanics* 134 (2006): 44-55.
12. Tanner, L.H. "The spreading of silicone oil drops on horizontal surfaces." *Journal of Physics: Applied Physics* 12(1979).
13. Bussman, M., S. Chandra, and J. Mostaghimi. "Modeling the splash of a droplet impacting on a solid surface." *Physics of Fluids, American Institute of Physics* Vol. 12.12(2000).
14. Fukai, J., Y. Shiiba, T. Yamamoto, O. Miyatake, D. Poulikakos, C.M. Megaridis, and Z. Zhao. "Wetting effects on the spreading of a liquid droplet colliding with a flat surface: Experiment and modeling." *American Institute of Physics, Physics of Fluids* 7.2(1995).
15. Pasandideh-Fard, M., Y.M. Qiao, and J. Mostaghimi. "Capillary effects during droplet impact on a solid surface." *American Institute of Physics, Physics of Fluids* 8.3(1996).
16. Guillou, S. and R. Makhloufi. "Effect of a shear-thickening rheological behavior on the friction coefficient in a plane channel flow: A study by Direct Numerical Solution." *Journal of non-Newtonian Fluid Mechanics* 144 (2007): 73-86.

17. Cheny, J.M. and K. Walters. "Rheological influences on the splashing experiment." *Journal of Fluid Mechanics* 86 (1999): 185-210.
18. Pascal, H. "Similarity solutions to some unsteady flows of non-Newtonian Fluids of Power Law Behavior." *International Journal of Non-Linear Mechanics* 27.5 (1992): 759-771.
19. Riazi, M.R. *Characterization and properties of petroleum fractions*. First Edition. West Conshohocken, PA: ASTM International, 2005.
20. "Diesel Fuel Exhaust and Emissions: Environmental Health Criteria 171." A draft report of United Nations Environment Program.

Tables

Table 2.1 Physical properties of liquids

Liquid	Density at 20 °C (kg/m³)	Viscosity at 20 °C (mPa-s)	Surface tension at 20 °C (mN/m)
Diesel	~830	3.61 (25 °C)	~28.0
Iso-butanol	805	3.77 (25 °C)	24.0
Glycerol	~1200	~1500	63.0

Source: Journal of Chemical Data, 1998 43(3)

Table 2.2 Concentrations and viscosities of the liquid blends

Polymer in diesel (Concentration %)	Base viscosity (cP)	Glycerol in iso-butanol (Concentration %)	Viscosity (cP)
0.5	4.33	3.8	4.44
1.0	6.1	14.53	6.23
1.4	19.375	36.1	19.5
2.0	39.3	47.1	39.6

Figures

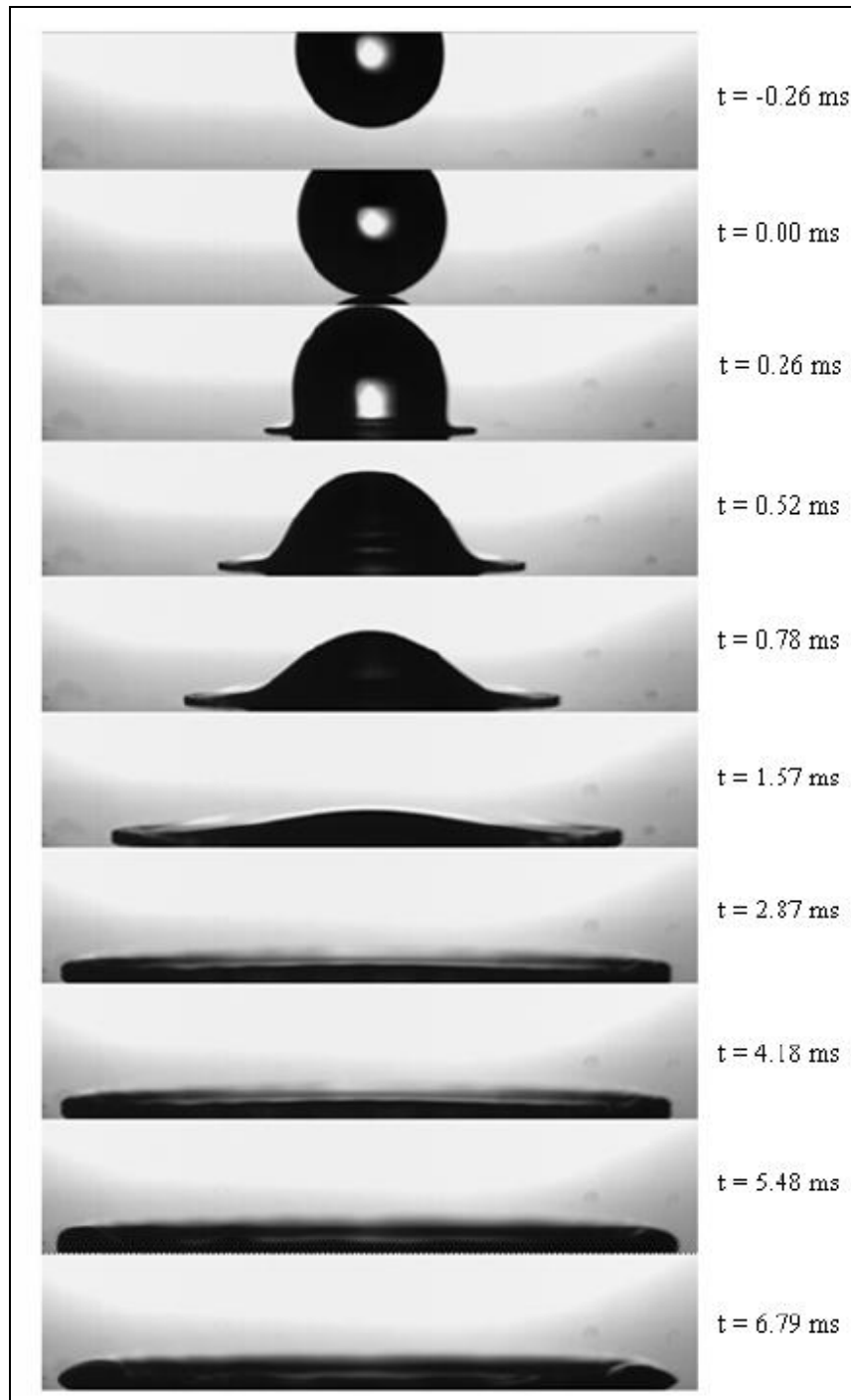
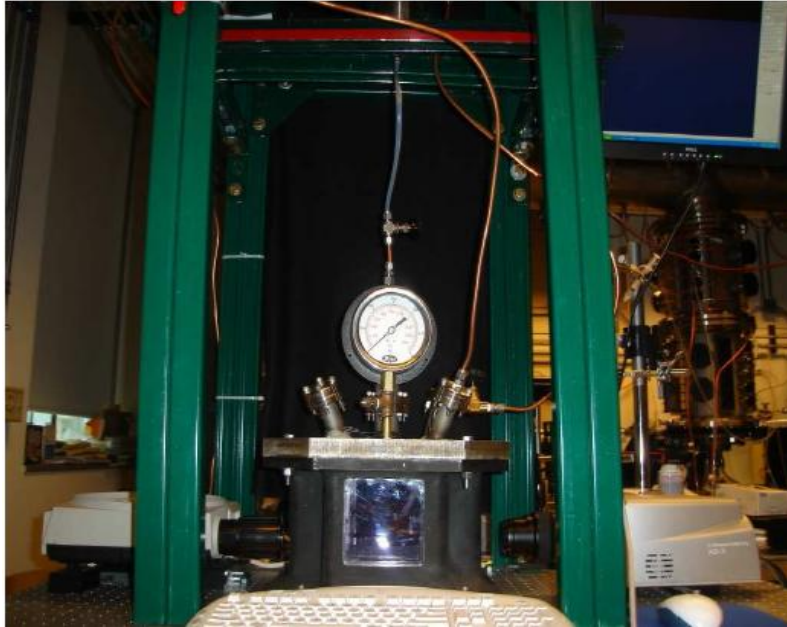
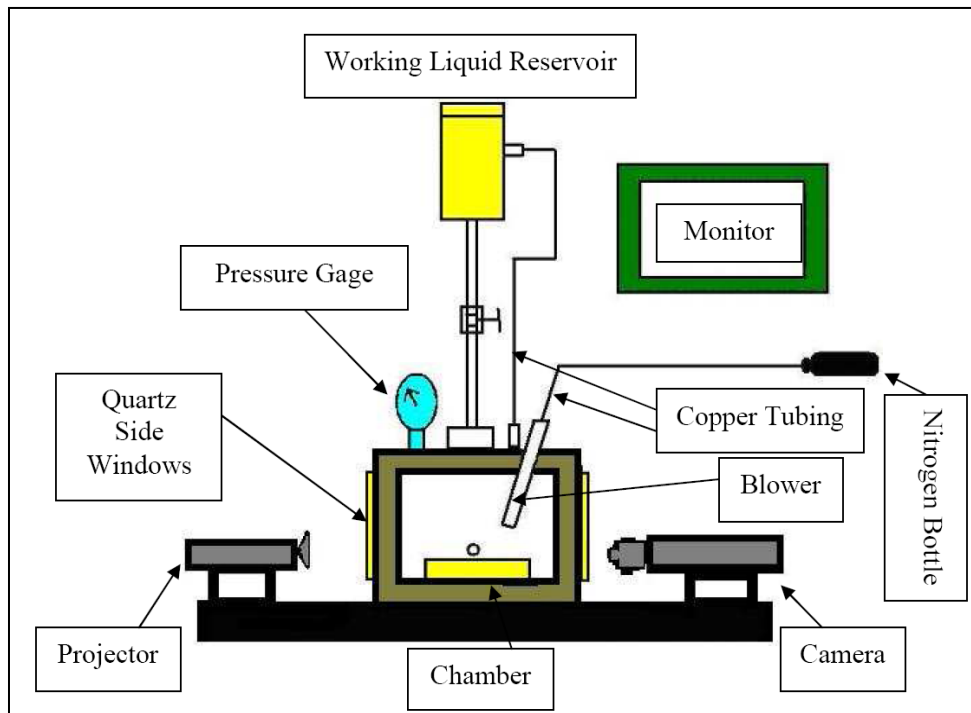


Fig. 2.1 Spreading of a liquid drop on a solid surface at atmospheric pressure



(a)



(b)

Fig. 2.2 The experimental arrangement: (a) actual set-up (b) schematic representation

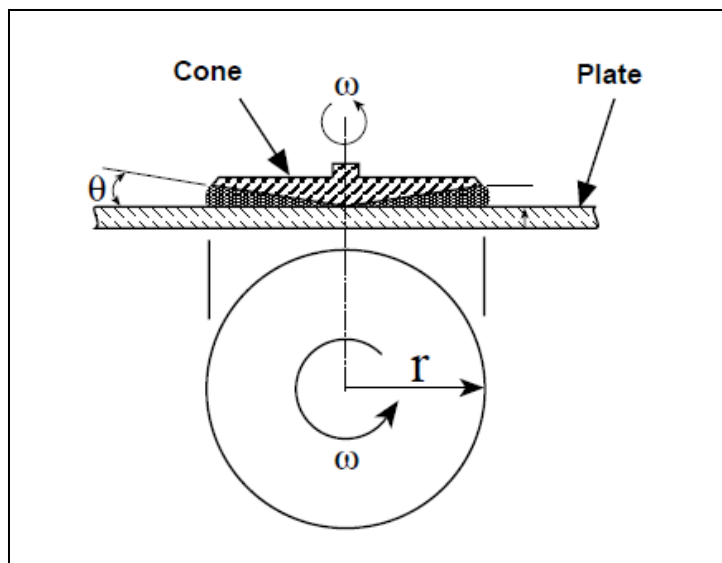


Fig. 2.3 Schematic representation of a cup and cone viscometer operation

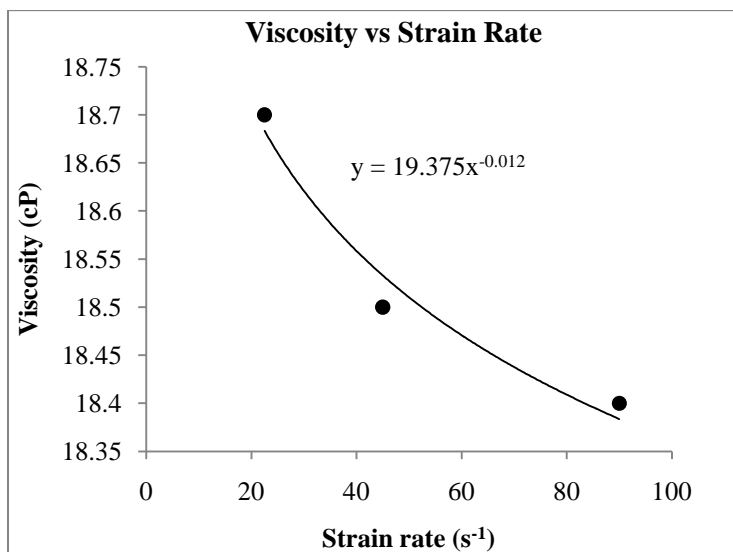


Fig. 2.4 Viscosity vs. strain rate for 1.4% polymer in diesel. Base viscosity is given by the coefficient of the fit, $\mu_0 = 19.375$ cP, $n = 1.012$

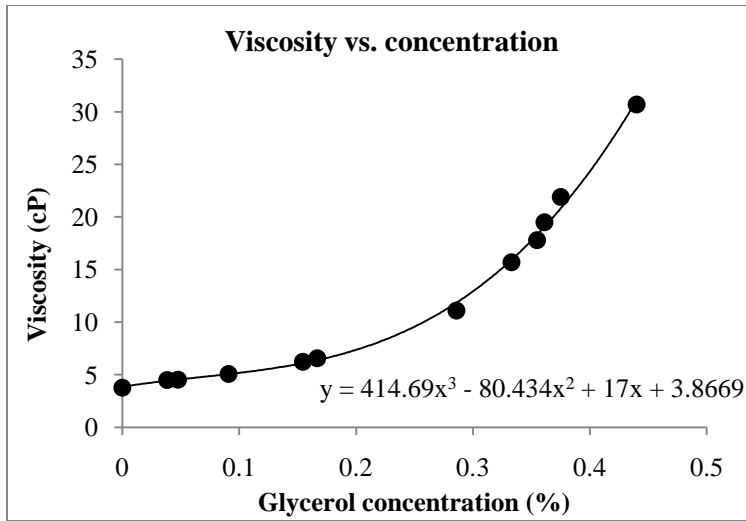


Fig. 2.5 Variation of viscosity of glycerol-isobutanol blend with glycerol %



Fig. 2.6 Diameter of the spreading lamella and diameter of the contact line

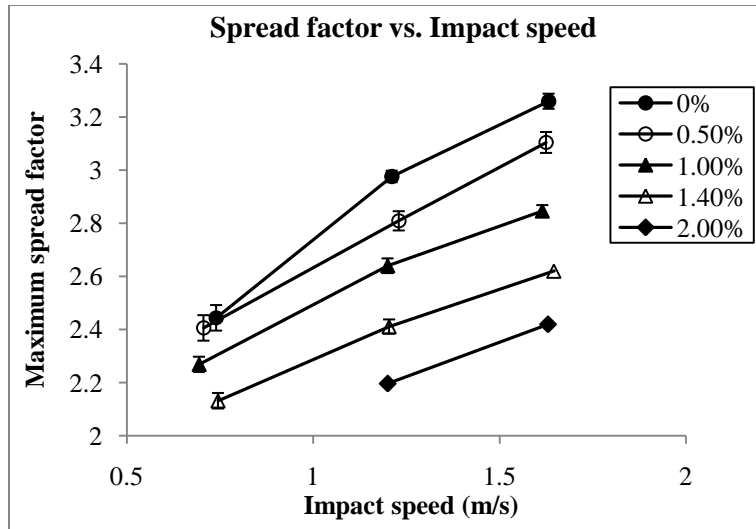


Fig. 2.7 Maximum spread factor vs. impact speed for different polymer concentrations.

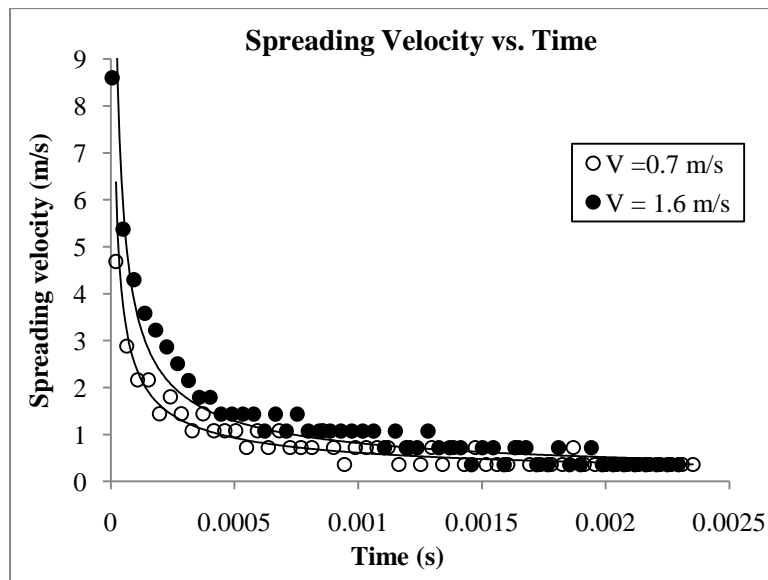


Fig. 2.8 Variation of spreading velocities with time for two diesel drops with $D_{eq} = 2.15$ mm

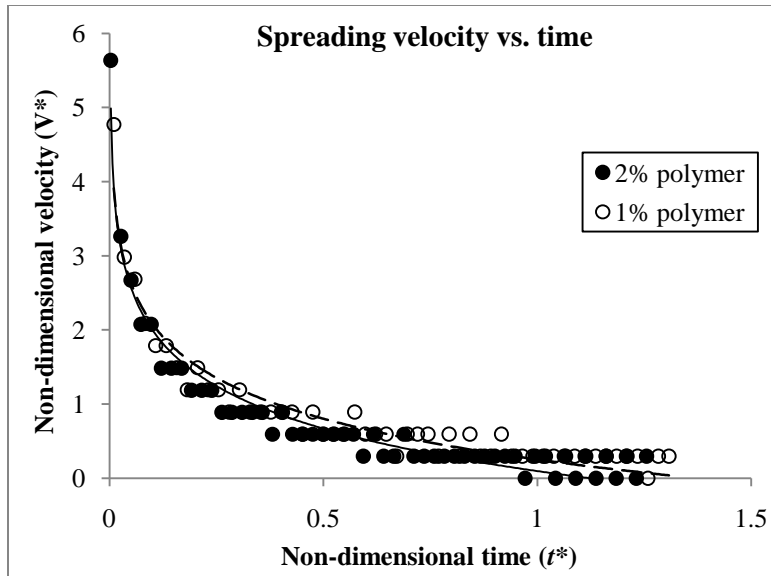


Fig. 2.9 Non-dimensional average spreading velocities vs. non-dimensional spread time for two polymer concentrations

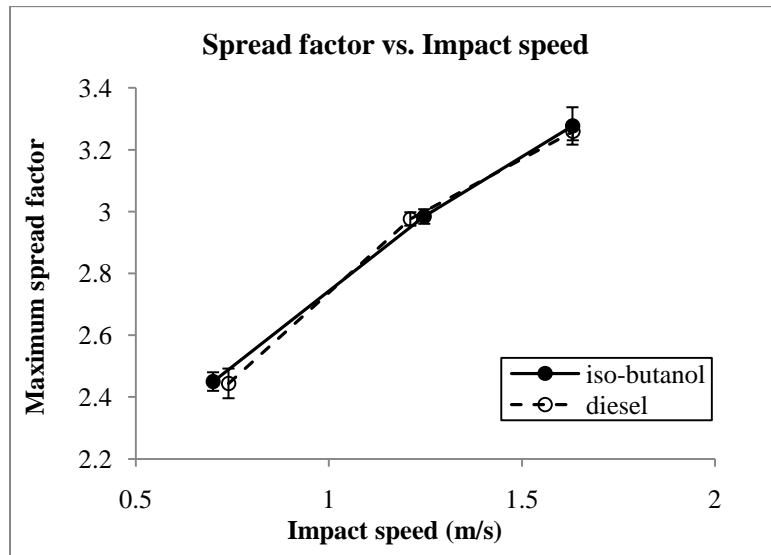


Fig. 2.10 Maximum spread factor vs. speed for diesel and iso-butanol

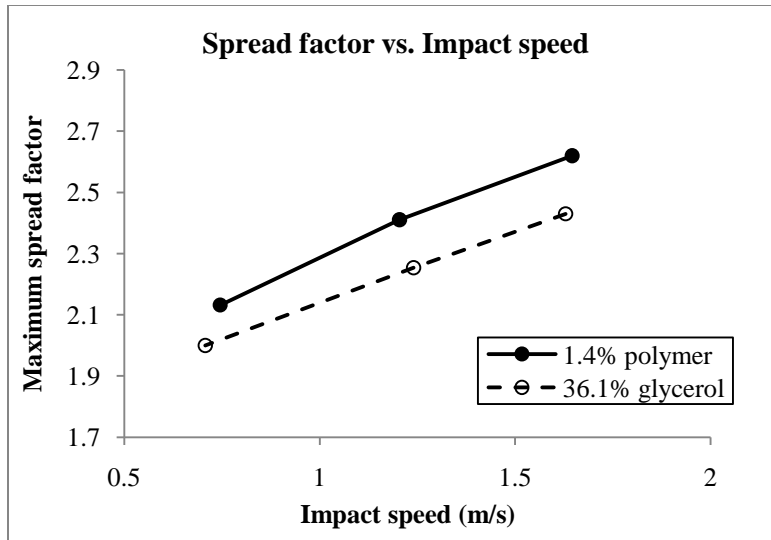


Fig. 2.11 Comparison of maximum spread factor for 1.4% diesel-polymer blend and 36.1% glycerol-isobutanol mixture

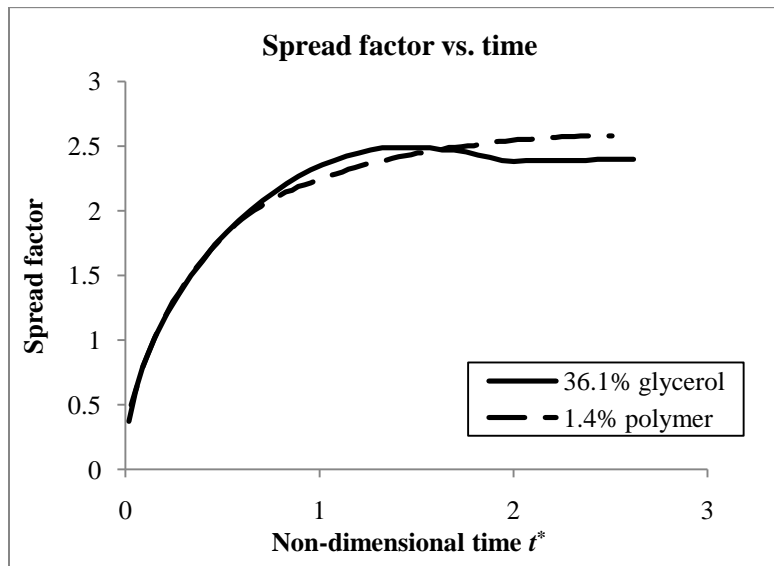


Fig. 2.12 Evolution of spread factor with non-dimensional time for polymer-diesel and glycerol-isobutanol blends

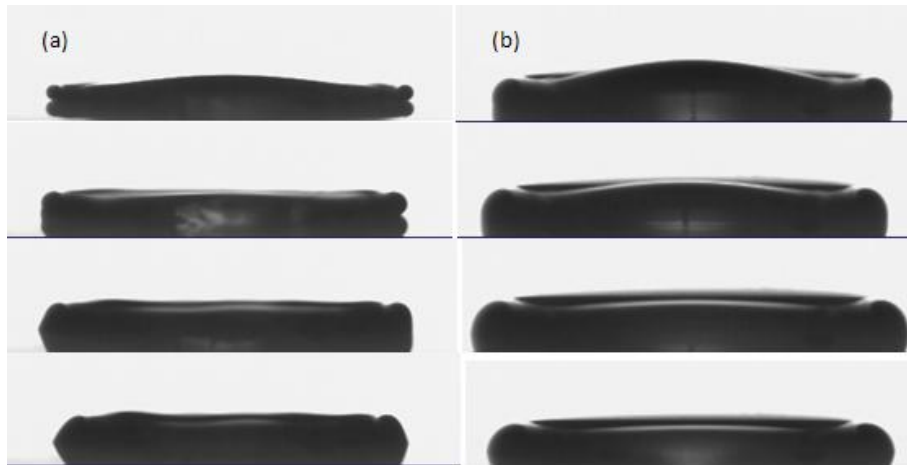


Fig. 2.13 Spreading near the maximum diameter (a) glycerol-isobutanol blend (b) polymer-diesel blend

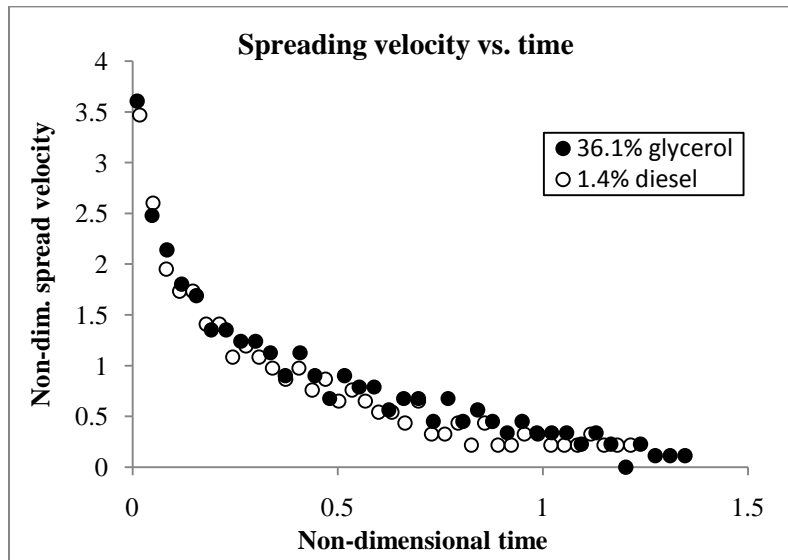


Fig. 2.14 Comparison of variation of spreading velocities with time for the two liquid blends

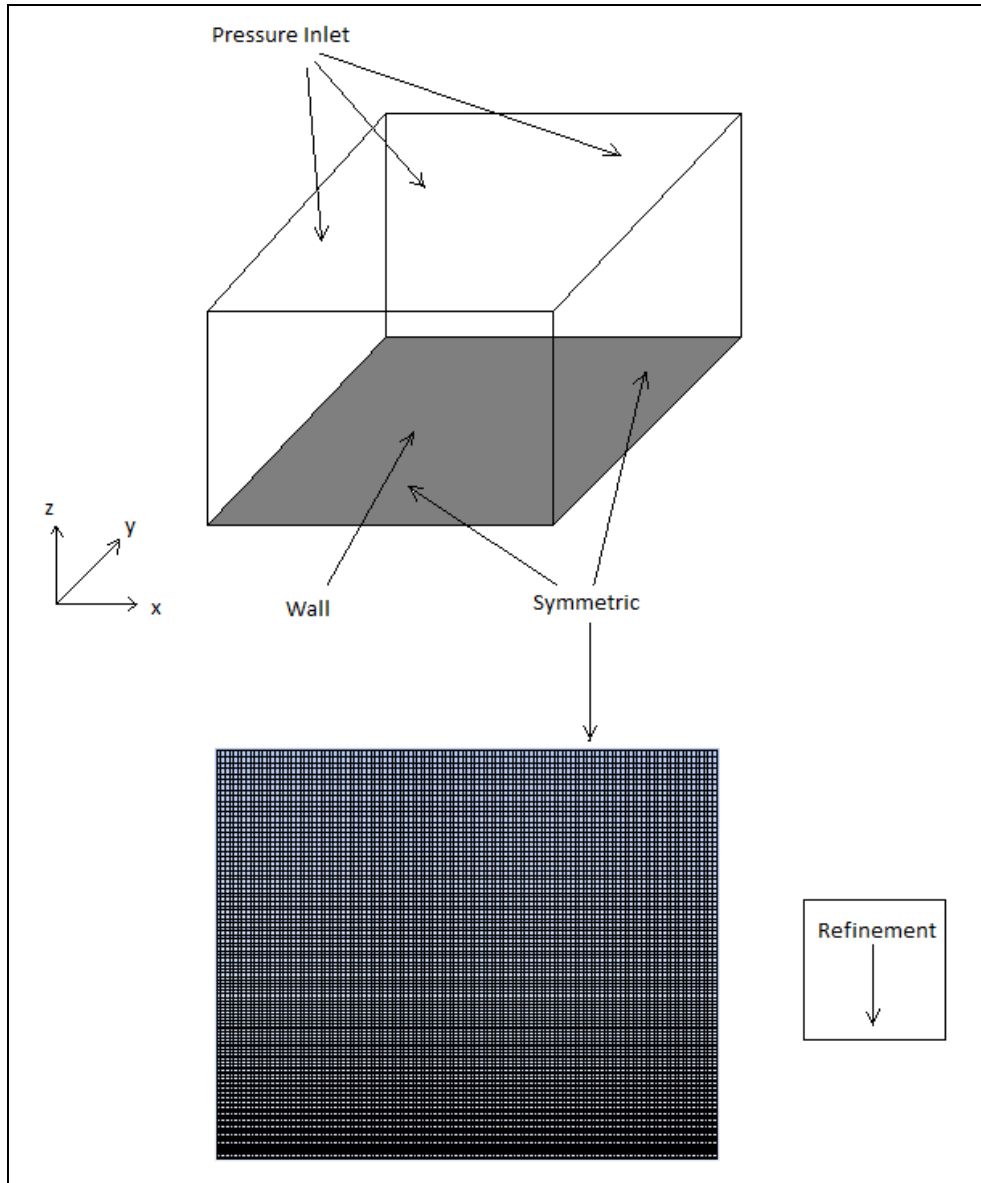


Fig. 3.1. Solution domain, boundary conditions and grid used in the simulations of drop impact on a horizontal surface

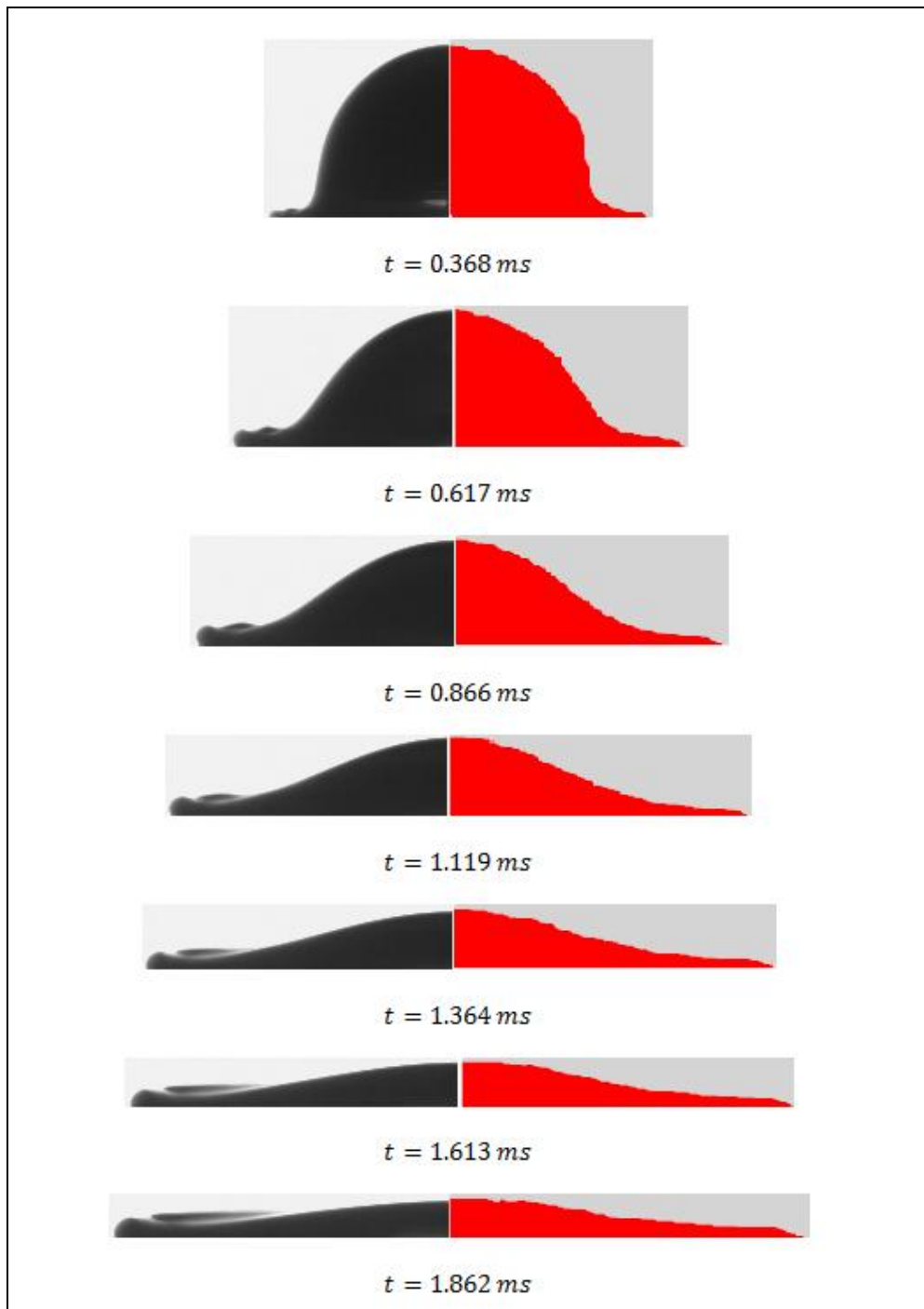


Fig. 3.2. Comparison of drop shape with time between experiments (left) and simulation (right) for a diesel drop of $D_{eq} = 2.16 \text{ mm}$ and $V_0 = 1.6 \text{ m/s}$

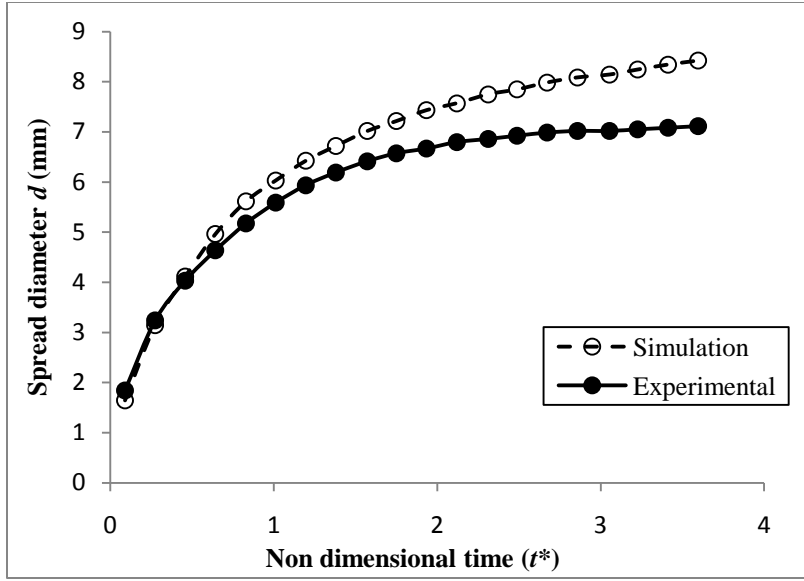


Fig. 3.3. Comparison of the experimental and numerical spread diameters of a diesel drop with $D_{eq} = 2.16$ mm and $V_0 = 1.6$ m/s on a horizontal surface ($SCA = 17.9^\circ$).

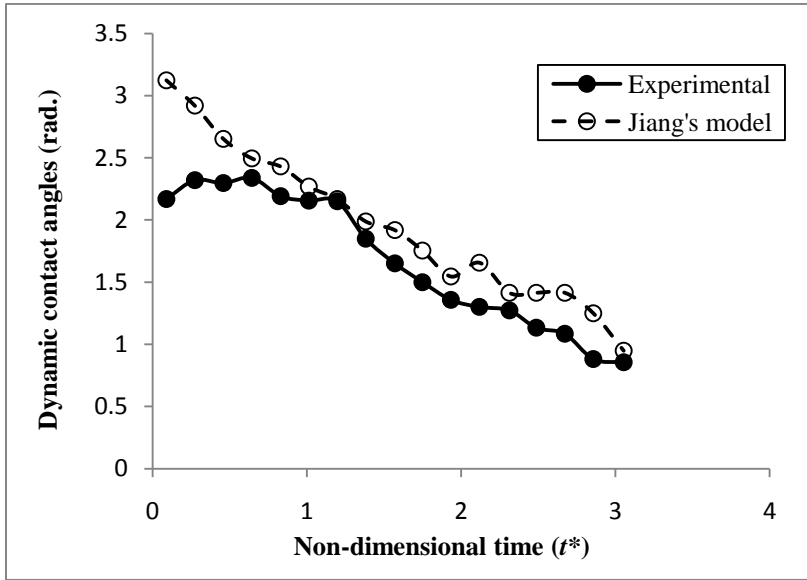


Fig. 3.4. Comparison between the dynamic contact angles as measured from experiments and as predicted by Jiang's model for a diesel drop with $D_{eq} = 2.16$ mm and $V_0 = 1.6$ m/s

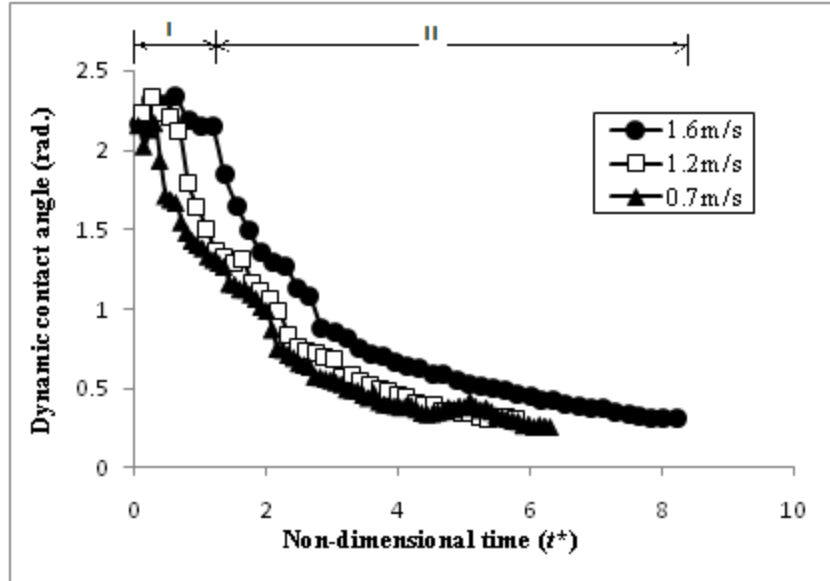


Fig. 3.5. Experimental values of dynamic contact angles for diesel drops impacting at three different impact speeds